Volume 1 | Number 1 | Jan 2013 | Pages 1–100

**ChemComm**

Chemical Communications
www.rsc.org/chemcomm

ROYAL SOCIETY OF CHEMISTRY

ROYAL SOCIETY OF CHEMISTRY

www.rsc.org/chemcomm

# ChemicalCommunications <sup>ChemComm</sup>

**Communication**

# P-type Ti(IV)-Based Metal-Organic Framework with Visible-Light Photo-Response

**Junkuo Gao,[a] Jianwei Miao,[b] Pei-Zhou Li,[c] Wen Yuan Teng,[a] Ling Yang,[a] Yanli Zhao,[c] Bin Liu,*[b] and Qichun Zhang*[a]**

**Here, we report a new Ti(IV)-based porous metal-organic framework (MOF) (NTU-9), which displayed strong absorption in the visible region with the bandgap of 1.72 eV.**
10 **The electronic structure and bandgap were furthermore investigated by DFT calculation. Photoelectrochemical studies indicated that NTU-9 is photoactive under visible light illumination ($\lambda > 400$ nm) and acts as a p-type semiconductor. The results demonstrated that Ti(IV)-based**
15 **MOFs could be promising visible-light photocatalysts for energy conversion and environmental remediation.**

Exploring new visible-light-driven photocatalysts has been one of the most attractive topics to address energy problem and reduce environmental contamination.[1] Because of its good photostability,
20 low cost, high efficiency, low toxicity and large abundance, titanium dioxide ($TiO_2$) have become one of the most studied semiconductors for photocatalysis.[2] However, its large bandgap has limited its application only in UV light range, which accounts for only 5% of the solar spectrum. Therefore, it is essential to
25 extend the optical response of $TiO_2$ into visible light through the modification of $TiO_2$ with inorganic or organic species.[3] However, most of such composites suffer from either poor stability or fast recombination. To address these problems, metal-organic frameworks (MOFs) might be a possible solution because
30 of their large surface areas and downsized catalytic centers (one metal or small metal-oxide cluster). Moreover, the surface areas, bandgaps and photoactivities of MOFs can be tuned through the change of organic ligands or metal centers.[4] In fact, some MOFs such as **MOF-5**, **UIO-66**, **MIL-100(Fe)**, and **MIL-88B(Fe)** have
35 already been demonstrated to have semiconductor properties for photoeletronics and photocatalysis.[5] Very recently, the successful demonstration of **MIL-125**[6] and its $NH_2$-functionalized isostructure (**MIL-125-NH2**) in light-driven water splitting and $CO_2$ reduction makes Ti-based MOFs more attractive as
40 photocatalyst.[7] However, it is worthy to note that no other Ti(IV)-based porous MOF structure except **MIL-125** has been reported. Here, we report a new porous Ti(IV)-based MOF structure (**NTU-9**), whose absorption reaches up to 750 nm and shows p-type semiconductor behaviour. **NTU-9** was obtained as red,
45 hexagonal prism crystals by reacting Ti(i-OPr)$_4$ (Titanium isopropoxide) with H$_4$DOBDC (2,5-Dihydroxyterephthalic acid) in acetic acid. Single crystal XRD analysis reveals that **NTU-9** crystallizes in the trigonal space group *P-31c*.[‡] As shown in Figure 1a, Ti atom is octahedrally coordinated with six oxygen
50 atoms from hydroxide and carboxylate groups. The bond length between Ti and the oxido oxygen atom is ~ 1.858 Å while the distance between Ti and oxygen atom from carboxylate group is ~2.037 Å. The coordination geometries of Ti center resemble the structure of [Ti(salicylate)$_3$]$^{2-}$ ions.[8] Note that the Ti-O bonds in
55 **NTU-9** are much shorter than the metal-O bonds in **MOF-74**[9] which is constituted of divalent metal ions (such as $Co^{2+}$, $Fe^{2+}$, $Mg^{2+}$) and DOBDC ligand, indicating the stronger bonding between Ti(IV) and O atoms. The connection between Ti(IV) atoms and DOBDC ligands forms a two dimensional (2-D)
60 honeycomb-like layer. These layers are stacked along the c-axis. There exist one dimensional (1-D) channels about 11 Å × 11 Å along the c-axis, which are similar to the 1-D channels in **MOF-74** (Figure 1c).[9b] All uncoordinated O atoms from the carboxylate groups point to the 1-D channels. The framework
65 {Ti$_2$(HDODBC)$_2$(H$_2$DOBDC)}$_n$ is neutral, and the empty spaces in channels are occupied by 2-propanol molecules. After removing guests in the channels, the solvent-accessible void in the structure of **NTU-9** is about 50.7 % calculated from PLATON. Thermogravimetric analysis (TGA) of **NTU-9**
70 revealed that most of the guest molecules in the channels were removed below 100 °C (Figure S1 in Electronic Supplementary Information). Crystalline **NTU-9** is stable in air, water and common organic solvents. After removing of the guest molecules (treated at 120 °C for 12 h under vacuum), the crystalline
75 structure of **NTU-9** was kept which was confirmed via the powder XRD pattern (Figure S2 in Electronic Supplementary Information). Details of the crystal structure and refinement data are provided in the supporting information (Table S1 in Electronic Supplementary Information). The experimental powder
80 XRD pattern for **NTU-9** matches very well with the simulated one (generated on the basis of single crystal structure analysis), which confirmed the phase purity of the bulk materials (Figure S2 in Electronic Supplementary Information).

The diffuse reflectance spectra were recorded on a PerkinElmer
85 Lambda 750s UV-Vis spectrometer. As shown in Figure 2, the spectrum of **NTU-9** shows a broad range of absorption in the visible from 400 nm to 750 nm with an absorption peak centered at around 520 nm. The calculated bandgap of **NTU-9** from the absorption onset is about 1.72 eV. The absorption of **NTU-9** was
90 dramatically red-shifted when compared with $TiO_2$ (3.2 eV for

anatase and 3.0 for rutile), and the reported Ti(IV)-based MOF **MIL-125** (3.6 eV) and its isostructure **MIL-125-NH2** (2.6 eV).[7c]
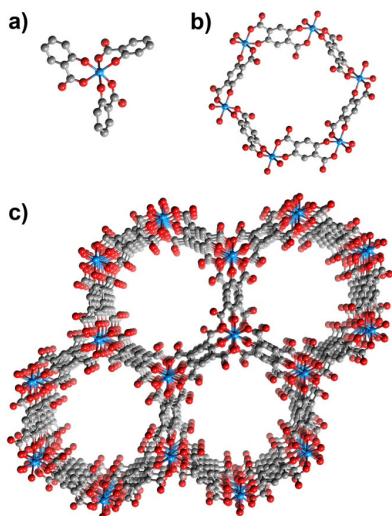


Figure 1. a) The coordination mode of Ti atom in **NTU-9**. b). The coordination of DOBDC ligand in **NTU-9**. c). 1-D channels of **NTU-9** viewed along the c-axis. Color representation: red, O; gray, C; blue, Ti. H atoms are removed for clarity.
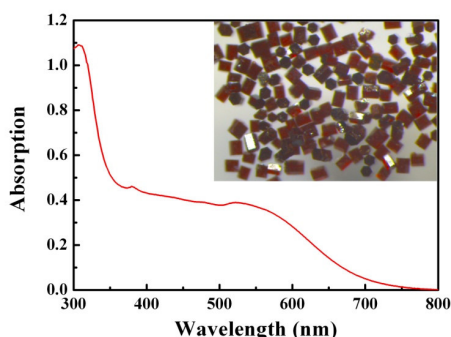


**Figure 2.** Diffuse reflectance spectra of **NTU-9**.

To understand the electronic structure of **NTU-9**, the density of states (DOS) and electronic band structure of **NTU-9** were calculated using the density functional theory (DFT) in CASTEP program.[10] As depicted in Figure S4-S6, the valence band (VB) of **NTU-9** between the energy level -4.0 eV and the Fermi level (0.0 eV) are mainly contributed from the O 2p states mixed with a small amount of C 2p states. The conduction band (CB) above Fermi energy are mostly made up of Ti 3d states, with minor contributions from the C 2p and O 2p states. The DOS results indicate the existence of charge transfer from the organic ligand to Ti(IV) atoms in **NTU-9**. The dominations of VB and CB by O and Ti atoms in **NTU-9** are similar to that of $TiO_2$, whose VB is mainly formed by the overlapping of O 2p orbitals and CB is mainly constituted of the 2d states of $TiO_2$. The small contributions of p atomic orbitals of carbon to the CB in **NTU-9** may alter and further reduce the band gap by changing the degree of conjugation or functional group modification in the ligands. This 'designable' character of MOFs could lead to the synthesis of more Ti(IV)-based MOF semiconductors with visible light activity. The CB minimum (1.74 eV) and VB maximum (0 eV) are located at the same k-point in the Brillouin zone (Figure S4).

The band structure illustrates that the interband transitions of **NTU-9** are direct, which may exhibit higher photonic efficiency compared with indirect band gap semiconductors such as $TiO_2$. The calculated energy band gap for **NTU-9** is 1.74 eV, which matches the experimental data very well.
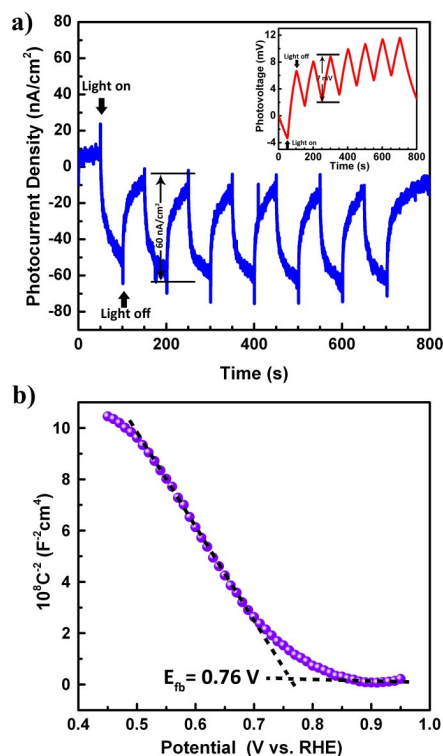


**Figure 3.** a). Zero-bias photocurrent response of **NTU-9**/FTO electrode upon chopped visible light illumination, inset is the photovoltage (illuminated open-circuit potential) responses of **NTU-9**/FTO electrode. b) Mott-Schottky plot of **NTU-9**/FTO electrode measured at a frequency of 1000 Hz. The flat-band potential of the NTU-9 is indicated by the intercept of the dashed lines.

The photoelectrochemical properties of **NTU-9** were studied in a three-electrode set-up. Figure 3a shows the photocurrent profile of **NTU-9**/FTO electrode recorded under zero-bias (two-electrode, short-circuit) condition, indicating that the **NTU-9** is active towards visible light ($\lambda$ > 400 nm) illumination. The repeatable cathodic (negative) photocurrent of ~ 60 $nA/cm^2$ suggests that **NTU-9** is a p-type semiconductor. As shown in the inset of Figure 3a, the **NTU-9**/FTO cells also showed highly repeatable photovoltage (illuminated open-circuit potential) responses of ~ 7 mV during the on-off cycles of illumination throughout the measurement. To further reveal the conductivity and flat-band potential of **NTU-9**, Mott-Schottky measurement was performed in 0.5 M $Na_2SO_4$ aqueous solution. As shown in Figure 3b, the negative slope indicates p-type behaviour of **NTU-9**, consistent with our previous analysis. Besides the p-type behavior, the Mott-Schottky measurement gives the flat-band potential of **NTU-9** at around 0.76 V vs. the reversible hydrogen electrode (RHE). The carrier concentration of **NTU-9** can be estimated from the slope of the Mott-Schottky plot using $N_a = (2/e_o\varepsilon\varepsilon_o)[d(1/C^2)/dV]^{-1}$, where $e_o$ is the electron charge, $\varepsilon$ is the **NTU-9** dielectric constant, $\varepsilon_o$ is the vacuum permittivity, and $N_a$ is the acceptor density. If we take the dielectric constant of **NTU-**

**9** to be ~ $10^1$ (a typical value for most of the MOFs)[11], the estimated carrier density of **NTU-9** is ~ $10^{15}$ $cm^{-3}$.

The visible photocatalytic activity of **NTU-9** was studied through the degradation of organic dyes. **NTU-9** showed good photocatalytic activity in degrading rhodamine B (RB) and methylene blue (MB) in aqueous solution under visible light irradiation ($\lambda > 420$ nm). Photodegradation of RB and MB were complete after 80 min and 20 min, respectively (Figure 4 and Figures S8-S10). During the 6 h testing period, **NTU-9** exhibited persistent high photoactivity and good photostability.
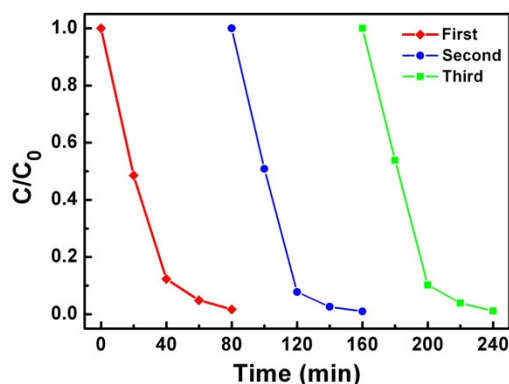


**Figure 4**. Recycling test on **NTU-9** for RB photo-degradation under visible light irradiation ($\lambda > 420$ nm).

In conclusion, we have reported a new Ti(IV)-based MOF, which absorbs visible photons up to 750 nm and shows a p-type semiconductor behavior. This new Ti(IV)-based MOF exhibits good photocatalytic activity and stability in degrading organic contaminants. Our results suggest that Ti(IV)-based MOFs could be promising candidates for the development of efficient visible light photocatalysts.

## Notes and references

*[a]School of Materials Science and Engineering, Nanyang Technological University, Singapore 639798, Singapore. E-mail: qczhang@ntu.edu.sg*
*[b]School of Chemical and Biomedical Engineering, Nanyang Technological University, Singapore 637459, Singapore. E-mail: liubin@ntu.edu.sg*
*[c]School of Physical and Mathematical Sciences, Nanyang Technological University, Singapore 637371, Singapore.*

† Electronic Supplementary Information (ESI) available: Experimental details, summary of crystal structure and refinement details of **NTU-9**, IR spectra, powder-XRD and TGA spectra of **NTU-9**. See DOI: 10.1039/b000000x/
‡Data collection of crystals was carried out on Bruker APEX II CCD diffractometer equipped with a graphite-monohromatized Mo-Kα radiation source ($\lambda$=0.71073 Å). Empirical absorption was performed, and the structure was solved by direct methods and refined with the aid of a SHELXTL program package. All hydrogen atoms were calculated and refined using a riding model. The **CCDC** number for **NTU-9** is 974959.

1. (a) S. Chu and A. Majumdar, *Nature*, 2012, **488**, 294; (b) G. D. Scholes, G. R. Fleming, A. Olaya-Castro and R. van Grondelle, *Nat. Chem.*, 2011, **3**, 763; (c) Y. Tachibana, L. Vayssieres and J. R. Durrant, *Nat. Photonics*, 2012, **6**, 511; (d) A. Kubacka, M. Fernández-García and G. Colón, *Chem. Rev.*, 2012, **112**, 1555.

2. (a) A. Fujishima and K. Honda, *Nature*, 1972, **238**, 37; (b) X. B. Chen, L. Liu, P. Y. Yu and S. S. Mao, *Science*, 2011, **331**, 746; (c) M. D'Arienzo, J. Carbajo, A. Bahamonde, M. Crippa, S. Polizzi, R. Scotti, L. Wahba and F. Morazzoni, *J. Am. Chem. Soc.*, 2011, **133**, 17652.

3. (a) X. X. Xu, C. Randorn, P. Efstathiou and J. T. S. Irvine, *Nat. Mater.*, 2012, **11**, 595; (b) M. D. Hernandez-Alonso, F. Fresno, S. Suarez and J. M. Coronado, *Energy Environ. Sci.*, 2009, **2**, 1231; (c) R. Asahi, T. Morikawa, T. Ohwaki, K. Aoki and Y. Taga, *Science*, 2001, **293**, 269; (d) F. Zuo, K. Bozhilov, R. J. Dillon, L. Wang, P. Smith, X. Zhao, C. Bardeen and P. Y. Feng, *Angew. Chem. Int. Ed.*, 2012, **51**, 6223.

4. (a) A. Corma, H. Garcia and F. X. L. Xamena, *Chem. Rev.*, 2010, **110**, 4606; (b) L. Q. Ma, J. M. Falkowski, C. Abney and W. B. Lin, *Nat. Chem.*, 2010, **2**, 838; (c) Y. J. Cui, Y. F. Yue, G. D. Qian and B. L. Chen, *Chem. Rev.*, 2012, **112**, 1126. (d) J. Gao, K. Ye, L. Yang, W.-W. Xiong, L. Ye, Y. Wang and Q. Zhang, *Inorg. Chem.*, 2014, DOI: 10.1021/ic402692p; (e) J. Gao, Q. Tay, W.-W. Xiong, P.-Z. Li, Y. Zhao, Z. Chen, and Q. Zhang, *Chem. Asian J.* 2014, **9**, 131; (f) J. Gao, M. He, Z. Y. Lee, W. Cao, W.-W. Xiong, Y. Li, R. Ganguly, T. Wu and Q. Zhang, *Dalton Transactions*, 2013, **42**, 11367; (g) J. Gao, K. Ye, M. He, W. Cao, W.-W. Xiong, Z. Y. Lee, Y. Wang, T. Wu; F. Huo, X. Liu and Q. Zhang, *J. Solid-State Chem.*, 2013, **206**, 27.

5. (a) F. X. Llabrés i Xamena, A. Corma and H. Garcia, *J. Phys. Chem. C*, 2007, **111**, 80; (b) C. G. Silva, A. Corma and H. Garcia, *J. Mater. Chem.*, 2010, **20**, 3141; (c) C. Wang, Z. G. Xie, K. E. deKrafft and W. L. Lin, *J. Am. Chem. Soc.*, 2011, **133**, 13445; (d) C. Y. Lee, O. K. Farha, B. J. Hong, A. A. Sarjeant, S. T. Nguyen and J. T. Hupp, *J. Am. Chem. Soc.*, 2011, **133**, 15858; (e) J. L. Wang, C. Wang and W. B. Lin, *Acs Catal.*, 2012, **2**, 2630; (f) C. G. Silva, I. Luz, F. X. L. I. Xamena, A. Corma and H. Garcia, *Chem. Eur. J.*, 2010, **16**, 11133.

6. M. Dan-Hardi, C. Serre, T. Frot, L. Rozes, G. Maurin, C. Sanchez and G. Ferey, *J. Am. Chem. Soc.*, 2009, **131**, 10857.

7. (a) T. Toyao, M. Saito, Y. Horiuchi, K. Mochizuki, M. Iwata, H. Higashimura and M. Matsuoka, *Catal. Sci. Technol.*, 2013, **3**, 2092; (b) Y. Horiuchi, T. Toyao, M. Saito, K. Mochizuki, M. Iwata, H. Higashimura, M. Anpo and M. Matsuoka, *J. Phys. Chem. C*, 2012, **116**, 20848; (c) C. H. Hendon, D. Tiana, M. Fontecave, C. Sanchez, L. D'arras, C. Sassoye, L. Rozes, C. Mellot-Draznieks and A. Walsh, *J. Am. Chem. Soc.*, 2013, **135**, 10942; (d) Y. Fu, D. Sun, Y. Chen, R. Huang, Z. Ding, X. Fu and Z. Li, *Angew. Chem. Int. Ed.*, 2012, **51**, 3364; (e) M. de Miguel, F. Ragon, T. Devic, C. Serre, P. Horcajada and H. Garcia, *Chemphyschem*, 2012, **13**, 3651; (f) M. A. Nasalevich, M. G. Goesten, T. J. Savenije, F. Kapteijn and J. Gascon, *Chem. Commun.*, 2013, **49**, 10575.

8. (a) K. Gigant, A. Rammal and M. Henry, *J. Am. Chem. Soc.*, 2001, **123**, 11632-11637; (b) K. Hong, W. Bak and H. Chun, *Inorg. Chem.*, 2013, **52**, 5645.

9. (a) N. L. Rosi, J. Kim, M. Eddaoudi, B. Chen, M. O'Keeffe and O. M. Yaghi, *J. Am. Chem. Soc.*, 2005, **127**, 1504; (b) P. D. C. Dietzel, Y. Morita, R. Blom and H. Fjellvag, *Angew. Chem. Int. Ed.*, 2005, **44**, 6354; (c) E. D. Bloch, W. L. Queen, R. Krishna, J. M. Zadrozny, C. M. Brown and J. R. Long, *Science*, 2012, **335**, 1606.

10. M. D. Segall, P. J. D. Lindan, M. J. Probert, C. J. Pickard, P. J. Hasnip, S. J. Clark and M. C. Payne, *J. Phys.: Condens. Matter.*, 2002, **14**, 2717.

11. (a) S. Eslava, L. P. Zhang, S. Esconjauregui, J. W. Yang, K. Vanstreels, M. R. Baklanov and E. Saiz, *Chem. Mater.*, 2013, **25**, 27; (b) W. Zhang, Y. Cai, R. G. Xiong, H. Yoshikawa and K. Awaga, *Angew. Chem. Int. Ed.*, 2010, **49**, 6608.

ChemComm Accepted Manuscript